Proceedings of the American Control Conference
Chicago, Illinois • June 2000

Full State Tracking and Internal Dynamics of Nonholonomic Wheeled Mobile Robots

Danwei Wang Guangyan Xu
School of Electrical and Electronic Engineering
Nanyang Technological University
Singapore 639798, edwwang@ntu.edu.sg

Abstract

Output tracking control and internal stability are analyzed for restricted mobile robots. Tracking error dynamics offers insights into the properties and stability of the input-output subsystem as well as the internal dynamics. Sufficient conditions for the full state tracking are developed. A type (1,1) mobile robot is studied in details and simulation results are presented to confirm the theory.

1 Introduction

In the last decade, feedback control for the trajectory tracking problem of nonholonomic wheeled mobile robots has been extensively studied based on the input-output dynamics [1, 2, 3, 4]. Especially, (static or dynamic) input-output feedback linearization is considered as a standard technique. However, few efforts were spent to analyze the nonlinear internal dynamic behaviors of those control schemes. One interesting observation was made in [5] on the internal stability of a 2-wheel differentially steered mobile robot. Its internal dynamics exhibits unstable properties when the mobile robot tracks a trajectory for backwards motion.

In this paper, we study the tracking error internal dynamics for general configurations of nonholonomic wheeled mobile robots. Our results provide the sufficient condition for the full state tracking stability by using the tracking control schemes based on the input-output dynamics. A special car-like robot is studied in details to enhance and visualize the results. The analysis to the car-like robot shows that the proposed sufficient condition is practical applicable by adjusting the parameters in the output function depending on the behavior of the desired trajectory.

2 Dynamics and Formulation

We consider wheeled mobile robots moving on a horizontal plane, as shown in Figure 1. The robots are

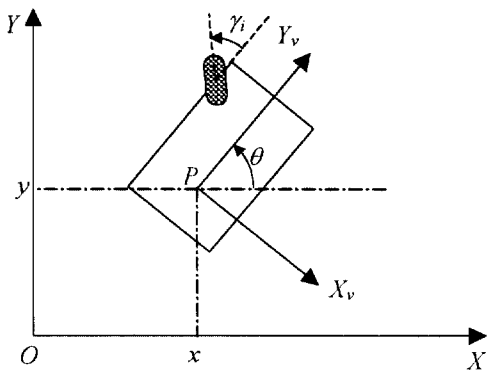

Figure 1: A mobile robot with steerable wheels

classified according to the mobility $1 \leq m \leq 3$ and the steerability $0 \leq s \leq 2$ as type (m, s) mobile robot [3]. If the robot is equipped with fixed and/or steering wheels, its mobility is restricted ($m \leq 2$) and the system is nonholonomic. Suppose there is no skidding between the wheels and the ground. The robot dynamics can be described as follows (an extension from [3]).

$$\dot{q} = G(q)\mu \quad (1)$$

$$\dot{\mu} = u \quad (2)$$

with

$$q = \begin{bmatrix} \zeta \\ \theta \\ \gamma \end{bmatrix} \quad \mu = \begin{bmatrix} v \\ \omega \end{bmatrix} \quad u = \begin{bmatrix} u_m \\ u_s \end{bmatrix} \quad G(q) = \begin{bmatrix} R^T(\theta)Q(\gamma) & 0 \\ b^T(\gamma) & 0 \\ 0 & I_s \end{bmatrix}$$

where, $\zeta = [x\ y]^T$ represent the coordinates of a reference point P on the robot in the inertial frame XOY. θ is the heading angle as defined in Figure 1. $\gamma = [\gamma_1 \cdots \gamma_s]^T$ represents the steering coordinates of independent steering wheels. Both vectors $v \in R^m$ and $\omega \in R^s$ are homogeneous to velocities. Both vectors $u_m \in R^m$ and $u_s \in R^s$ are control inputs homogeneous to torques. $R(\theta)$ is the standard rotation matrix. The matrix $Q(\gamma)$ and vector $b(\gamma)$ for each type of nonholonomic wheeled mobile robots are listed in Table 1. For the restricted mobile robot, the steering coordinate vector γ can be further partitioned as

$$\gamma = [\gamma^1 \quad \gamma^2]^T \qquad \forall\, \gamma^1 \in R^{m+s-2},\ \gamma^2 \in R^{2-m}$$

Table 1:

Type (m, s)	(2,0)	(2,1)	(1,1)	(1,2)
$Q(\gamma) \in R^{2\times m}$	$\begin{bmatrix} 1 & 1 \\ 0 & 0 \end{bmatrix}$	$\begin{bmatrix} \cos\gamma & 0 \\ \sin\gamma & 0 \end{bmatrix}$	$\begin{bmatrix} \cos\gamma \\ 0 \end{bmatrix}$	$\begin{bmatrix} \cos\gamma_1 \cos\gamma_2 \\ \sin(\gamma_1+\gamma_2)/2 \end{bmatrix}$
$b^T(\gamma) \in R^m$	$[-1 \quad 1]/a$	$[0 \quad 1]$	$\sin\gamma/a$	$\sin(\gamma_1-\gamma_2)/2a$
$\gamma^1 \in R^{m+s-2}$	null	γ	null	γ_1
$\gamma^2 \in R^{2-m}$	null	null	γ	γ_2
$d(\gamma) \in R^2$	$\begin{bmatrix} l \\ 0 \end{bmatrix}$	$\begin{bmatrix} l \\ 0 \end{bmatrix}$	$\begin{bmatrix} a + l\cos(p\gamma) \\ l\sin(p\gamma) \end{bmatrix}$	$\begin{bmatrix} a + l\cos(\gamma_2) \\ l\sin(\gamma_2) \end{bmatrix}$
Regular conditions	$l \neq 0$	$l \neq 0$ $\lvert\gamma\rvert < \frac{\pi}{2}$	$lp \neq 0$ $\lvert l-p\rvert < \frac{\pi}{2\gamma_{max}}$ $\lvert\gamma\rvert < \gamma_{max} < \frac{\pi}{2}$	$l \neq 0$ $\lvert\gamma_2\rvert < \frac{\pi}{2}$

Since $0 \leq m+s-2 \leq 1$ and $0 \leq 2-m \leq 1$ must be valid, both γ^1 and γ^2 are either a scalar or a null. Then, we define the output function as follows.

$$z = h(q) = \begin{bmatrix} \zeta + R^T(\theta)d(\gamma) \\ \gamma^1 \end{bmatrix} \tag{3}$$

where, vector γ^1, γ^2 and $d(\gamma)$ for each type of robot are given by Table 1. Note that, the first two entries of z represents a virtual reference point in the XOY plane. This output function is such defined that it may be decoupled to input u, i.e., the following decoupling matrix

$$E(q) = \frac{\partial h(q)}{\partial q} G(q) = \begin{bmatrix} R^T(\theta) & 0 \\ 0 & I_{m+s-2} \end{bmatrix} \bar{E}(\gamma) \tag{4}$$

with

$$\bar{E}(\gamma) = \begin{bmatrix} Q(\gamma) + \begin{bmatrix} 0 & -1 \\ 1 & 0 \end{bmatrix} d(\gamma) b^T(\gamma) & \frac{\partial d(\gamma)}{\partial \gamma} \\ 0 & \frac{\partial \gamma^1}{\partial \gamma} \end{bmatrix}$$

is nonsingular if the regular conditions in Table 1 are satisfied. Note that, parameters l and p in (3) have explicit physical meanings and can be selected at will. Moreover, the steering angles γ^1 and γ^2 are always restricted by the robot mechanism such that their maximums are smaller than 90 degree. Therefore, the regular conditions in Table 1 can always be satisfied for real restricted mobile robots.

The control task is to track a feasible desired trajectory $(q_d(t), \mu_d(t))$, which is pre-specified by an open-loop motion planner such that the dynamics (1)(2) are satisfied for a uniformly bounded input $u_d(t)$ and corresponding uniformly bounded velocity $\mu_d(t)$, i.e.,

$$\dot{q}_d = G(\theta_d, \gamma_d)\mu_d \tag{5}$$

$$\dot{\mu}_d = u_d \tag{6}$$

Clearly, the desired trajectory can also be expressed in the form of output (3) as

$$z_d = h(q_d) \tag{7}$$

Since the same structure between system (1)(2) and the trajectory (5)(6), one may establish the full order dynamics in terms of the state tracking error $\tilde{q} = q - q_d$ and $\tilde{\mu} = \mu - \mu_d$. We say that the system (1)(2) achieves *stable full state tracking* to trajectory (5)(6) if a control law u makes the full order dynamics of $(\tilde{q}, \tilde{\mu})$ uniformly stable. Similarly, since the system (1)-(3) is input-output decoupled, one may establish the input-output dynamics in terms of the output tracking error $\tilde{z} = z - z_d$. We say that the system (1)-(3) achieves *stable output tracking* to trajectory (7) if a control law u makes the input-output dynamics of $\tilde{z}$ uniformly stable.

We should note that the output function $h(q)$ in (3) is an epimorphism. So, the stable full state tracking implies the stable output tracking. However, the reverse might not be true. It is understood that, for a given trajectory $z_d(t)$, the generalized states $q_d(t)$ might not be unique, e.g., a straight line motion of $z_d(t)$ may be caused by forward or backward motion of a mobile robot and corresponds to different solutions of generalized states $q_d(t)$ and $\mu_d(t)$. In the extreme case, the output tracking of $z_d(t)$ may require the solution of $q_d(t)$ getting out of its admissible range. For instance, steering angle γ is required to have a value out of its physical limitation, such that the output tracking control design is not implementable. Next, we shall show that controllers, which stabilize the input-output dynamics of $\tilde{z}$, may achieve the stable full state tracking under certain condition.

3 Full state tracking

Since the decoupling matrix $E(q)$ is nonsingular, one may check that, by defining a function

$$\eta = k(q) = [\theta \quad \gamma^2]^T \tag{8}$$

the following maps

$$\begin{bmatrix} \xi_1 \\ \eta \end{bmatrix} = \Phi(q) = \begin{bmatrix} h(q) \\ k(q) \end{bmatrix} \tag{9}$$

and

$$\begin{bmatrix} \xi_1 \\ \xi_2 \\ \eta \end{bmatrix} = \bar{\Phi}(q,\mu) = \begin{bmatrix} h(q) \\ \dot{h}(q) \\ k(q) \end{bmatrix} = \begin{bmatrix} h(q) \\ E(q)\mu \\ k(q) \end{bmatrix} \tag{10}$$

are both diffeomorphisms. Clearly, $\Phi(\cdot)$ and $\bar{\Phi}(\cdot)$ also map the desired trajectory (1)(2) to the one in the new coordinates $(\xi_{1d}, \xi_{2d}, \eta_d)$.

Define tracking errors $\tilde{\xi} = \xi_i - \xi_{id}$ $(i = 1, 2)$, $\tilde{\eta} = \eta - \eta_d$, and $\tilde{z} = z - z_d$. One may find a feedback u such that the dynamics of tracking errors can be obtained as follows

$$\dot{\tilde{\xi}}_1 = \tilde{\xi}_2 \tag{11}$$

$$\dot{\tilde{\xi}}_2 = g(\tilde{\xi}_1, \tilde{\xi}_2) \tag{12}$$

$$\dot{\tilde{\eta}} = \varphi(\tilde{\xi}_1, \tilde{\xi}_2, \tilde{\eta}, t) \tag{13}$$

$$\tilde{z} = \tilde{\xi}_1 \tag{14}$$

where,

$$\begin{aligned} \varphi(\tilde{\xi}_1, \tilde{\xi}_2, \tilde{\eta}, t) = {} & F(\tilde{\xi}_1 + \xi_{1d}(t), \tilde{\eta} + \eta_d(t))(\tilde{\xi}_2 + \xi_{2d}(t)) \\ & - F(\xi_{1d}(t), \eta_d(t))\xi_{2d}(t) \end{aligned} \tag{15}$$

and

$$F(\cdot) = \left. \frac{\partial k(q)}{\partial q} G(q) E^{-1}(q) \right|_{q=\Phi^{-1}(\cdot)} \tag{16}$$

This set of tracking error dynamic equations (11)-(14) consists of two parts. The first part is the ξ-subsystem (11)(12), which characterizes the input-output dynamics. The second part is the η-subsystem (13), which is not controllable and characterizes the internal dynamics. In the case that the input-output dynamics ξ-subsystem is stabilized, the stability of internal dynamics η-subsystem determines whether the stable full state tracking and even the stable output tracking can be achieved. In particular, the zero dynamics, equation (13)(15) when the system output is set to zero ($\tilde{z} = 0$), is given as

$$\begin{aligned} \dot{\tilde{\eta}} &= \varphi_o(\tilde{\eta}, t) \\ &= [F(\xi_{1d}(t), \tilde{\eta} + \eta_d(t)) - F(\xi_{1d}(t), \eta_d(t))]\, \xi_{2d}(t) \end{aligned} \tag{17}$$

and its stability is critical to the internal stability. To gain more insights to the tracking error zero dynamics, by using (16) and (4), (17) can be expressed in terms of the original mobile robot generalized coordinates as

$$\begin{aligned} \dot{\tilde{\eta}} &= f_o(\tilde{\eta}, \gamma_d, \mu_d) \\ &= \begin{bmatrix} b^T(\gamma_d^1, \tilde{\gamma}^2 + \gamma_d^2) & 0 & 0 \\ 0 & 0 & I_{2-m} \end{bmatrix} \bar{E}^{-1}(\gamma_d^1, \tilde{\gamma}^2 + \gamma_d^2) \cdot \\ & \begin{bmatrix} R(\tilde{\theta}) & 0 \\ 0 & I_{m+s-2} \end{bmatrix} \bar{E}(\gamma_d)\mu_d - \begin{bmatrix} b^T(\gamma_d) & 0 & 0 \\ 0 & 0 & I_{2-m} \end{bmatrix} \mu_d \end{aligned} \tag{18}$$

Here, we may give a main result by the following theorem.

Theorem 1 *Consider the tracking problem of robot (1)(2) to a moving desired trajectory (q_d, μ_d) satisfying (5)(6) with $\gamma_d(t)$ $\mu_d(t)$, and $u_d(t)$ uniformly bounded.*

(a) Suppose that control input u is specified such that, by using the transformation (10), the closed-loop ξ-subsystem (11)(12) is stable.

(b) Furthermore, by denoting

$$A(\gamma_d, \mu_d) = \left. \frac{\partial f_o(\tilde{\eta}, \gamma_d, \mu_d)}{\partial \tilde{\eta}} \right|_{\tilde{\eta}=0} \tag{19}$$

suppose the linear system

$$\dot{\tilde{\eta}} = A(\gamma_d, \mu_d)\tilde{\eta} \tag{20}$$

for every frozen $(\gamma_d(t), \mu_d(t)) = (\bar{\gamma}_d, \bar{\mu}_d)$ is exponentially stable in a neighborhood of $\tilde{\gamma}^2 = 0$.

Then, the robot system (1)(2) locally achieves stable full state tracking to desired trajectory (5)(6).

Outline of proof: Because of the diffeomorphism (10), the proof can be completed by showing that suppositions (a)(b) imply the uniform stability of the tracking error dynamics (11)-(13). The proof consists of flowing two steps.

(i) f_o in (18) and hence $\partial f_o / \partial \tilde{\eta}$ is Lipschitz in $\tilde{\eta}$ in a neighborhood of $\tilde{\gamma}^2 = 0$, uniformly in t. So, (20) is the linear approximation of (18). Furthermore, since $\dot{\gamma}_d(t) = \omega_d(t) \in \mu_d$ and $\dot{\mu}_d(t) = u_d(t)$ are uniformly bounded, linear system (20) is a slowly time varying system by Lemma 2.44 in [6]. Therefore, supposition (b) locally implies the uniform asymptotic stability of the tracking error zero dynamics (18) and hence (17).

(ii) Noticing the structure of matrices $E(q)$, $G(q)$ and Table 1, $F(\cdot)$ is Lipschitz, uniformly in t. Furthermore, $\xi_{2d} = E(q_d)\mu_d$ is uniformly bounded. Then, $\varphi(\tilde{\xi}_1, \tilde{\xi}_2, \tilde{\eta}, t)$ is Lipschitz in $(\tilde{\xi}_1, \tilde{\xi}_2, \tilde{\eta})$, uniformly in t. Finally the claims follow Corollary in page 445 of [7] and the result (i). □

In the case that output tracking control law is used, Theorem 1 offers sufficient conditions for the stable full state tracking and thus the stable output tracking in a neighborhood of $\tilde{\eta} = 0$.

4 Tracking stability of a car-like robot

The stability analysis method proposed in Theorem 1 is generally suitable for analyzing the trajectory tracking stability of any wheeled mobile robot under an output tracking control scheme. Without loss of generality, we

investigate the car-like robot in Figure 2, whose dynamics is given by (1)(2) with elements of type (1,1) in Table 1. In this special case, v is the longitudinal velocity; ω is the steering rate; a is a positive constant of the wheelbase. Parameters (l, p) defines a virtual reference point P_r.

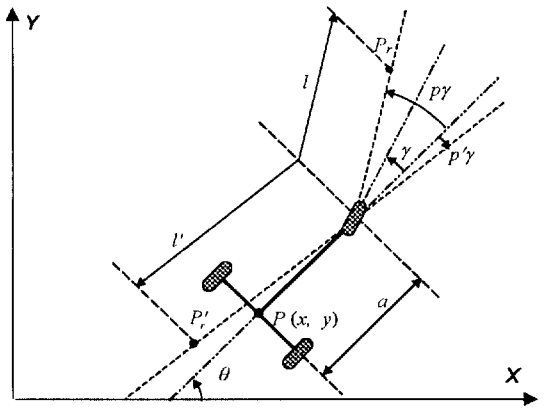

Figure 2: A car-like robot configuration

After some derivations, the linear approximation (20) of the car-like robot is obtained as

$$\dot{\tilde{\eta}} = \begin{bmatrix} a_{11}(\gamma_d, v_d, \omega_d) & a_{12}(\gamma_d, v_d, \omega_d) \\ a_{21}(\gamma_d, v_d, \omega_d) & a_{22}(\gamma_d, v_d, \omega_d) \end{bmatrix} \tilde{\eta} \qquad (21)$$

with

$$\begin{aligned}
a_{11} &= v_d \frac{2l\sin^2\gamma_d - a\cos(p\gamma_d - 2\gamma_d) + a\cos(p\gamma_d)}{a^2(\cos(p\gamma_d - 2\gamma_d) + \cos\gamma_d)} \\
&\quad + \frac{pl\omega_d \sin(2\gamma_d)}{a(\cos(p\gamma_d - 2\gamma_d) + \cos\gamma_d)} \\
a_{12} &= \frac{2v_d pl\sin^2\gamma_d + 2v_d a\cos(p\gamma_d) + p^2 la\omega_d \sin(2\gamma_d)}{a^2(\cos(p\gamma_d - 2\gamma_d) + \cos\gamma_d)} \\
a_{21} &= 2v_d \frac{la\cos(p\gamma_d - 2\gamma_d) - l^2\sin^2\gamma_d - a^2 - la\cos(p\gamma_d)}{pla^2(\cos(p\gamma_d - 2\gamma_d) + \cos\gamma_d)} \\
&\quad \omega_d \frac{a\sin(p\gamma_d) + a\sin(p\gamma_d - 2\gamma_d) - l\sin(2\gamma_d)}{a(\cos(p\gamma_d - 2\gamma_d) + \cos\gamma_d)} \\
a_{22} &= v_d \frac{a\cos(p\gamma_d - 2\gamma_d) - 2l\sin^2\gamma_d}{a^2(\cos(p\gamma_d - 2\gamma_d) + \cos\gamma_d)} \\
&\quad - v_d \frac{2a + l(2+p)\cos(p\gamma_d)}{pla(\cos(p\gamma_d - 2\gamma_d) + \cos\gamma_d)} \\
&\quad \omega_d \frac{pa\sin(p\gamma_d) + pa\sin(p\gamma_d - 2\gamma_d) - pl\sin(2\gamma_d)}{a(\cos(p\gamma_d - 2\gamma_d) + \cos\gamma_d)}
\end{aligned}$$

This linear approximation has 5 parameters $(\gamma_d, v_d, \omega_d, l, p)$. It is so complex that its eigenvalues analytic studies are, in general, difficult, if not impossible. However, in some special cases, eigenvalues analysis can offer more insights. One such case is given by setting $p = 1$ as

$$\begin{aligned}
A(\gamma_d, v_d) &= v_d \begin{bmatrix} 0 & \frac{1}{a} \\ -\frac{1}{l\cos\gamma_d} & -\frac{1}{l\cos\gamma_d} - \frac{1}{a} \end{bmatrix} \\
&\quad + \frac{l}{a^2}\sin\gamma_d (v_d \tan\gamma_d + a\omega_d) \begin{bmatrix} 1 & 1 \\ -1 & -1 \end{bmatrix}
\end{aligned}$$

its eigenvalues at every frozen $(\bar{\gamma}_d, \bar{v}_d)$ are

$$\lambda_1 = -\frac{\bar{v}_d}{a} \qquad \lambda_2 = -\frac{\bar{v}_d}{l\cos\bar{\gamma}_d} \qquad (22)$$

and both of them are negative if $\bar{v}_d, l > 0$ and $|\bar{\gamma}_d| < \pi/2$. Applying Theorem 1, we conclude that the stable full state tracking of a car-like robot to a feasible trajectory ($|\gamma_d| < \pi/2$, v_d, ω_d, u_d are uniformly bounded) that moves forwards ($v_d > 0$) can be achieved by choosing output function such that the virtual reference point P_r is in front of the front wheel axle ($l > 0$) in the steering direction ($p = 1$).

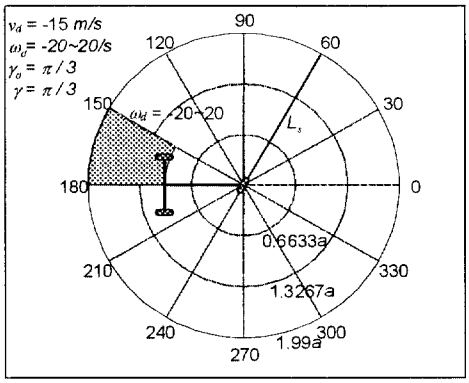

(a) High speed

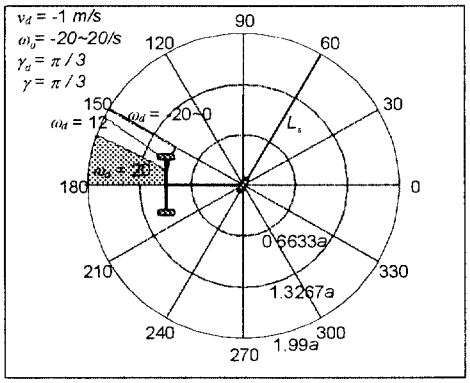

(b) Low speed

Figure 3: Backward moving stable sets

To further investigate the stable full state tracking problem of a car-like robot to a feasible trajectory that moves backwards ($v_d < 0$), eigenvalues analysis faces limitation. Here, we use numerical search to explore the sets of five design parameters $(v_d, \omega_d, \gamma_d, l, p)$ that ensure the full state tracking stability. In Figure 3, the shaded areas are the sets of locations of the virtual reference points ($l < -a$ and $p < 0$) that are able to ensure the stable full state tracking at different setting of $(\bar{\gamma}_d, \bar{\omega}_d, \bar{v}_d)$. Figure 3 shows that lower velocities or higher steering rates come with smaller parameter values of p. Note that such sets of virtual reference points are open sets and the boundaries do not guarantee the full state tracking stability.

The above analyses offer applicable sufficient conditions for the full state tracking of the car-like robot: (a) setting $l > 0$ and $p = 1$ when $v_d > 0$; (b) setting $l < -a$ and $p_\mu < p < 0$ with p_μ determined by the behavior of the desired trajectory,

i.e., with desired steering rate increasing and desired velocity decreasing, p_μ tends to zero.

5 Simulation results

In the simulation study, the desired trajectory consists of three straight lines and two curves. The first curve is designed with a maximum curvature $k_{max} = 0.5238$ and a maximum curvature change rate $\dot{k}_{max} = 0.6864$. The second curve has a higher maximum curvature $k_{max} = 0.8479$ and a much higher curvature change rate $\dot{k}_{max} = 1.7599$. In the following, we use a simple input-output feedback linearization control law to verify the analyses in the last section.

In the first case, the car-like robot is expected to move forward with the desired velocity of $v_d = 2$m/sec. The virtual reference point is chosen at $P_0 = (l, p) = (0.5a, 1)$. Based on Theorem 1, the linear approximation (21) of the tracking error zero dynamics is asymptotically stable and so is the robot tracking. The simulation result, as shown in Figure 4, confirms that the vehicle follows the desired trajectory through out.

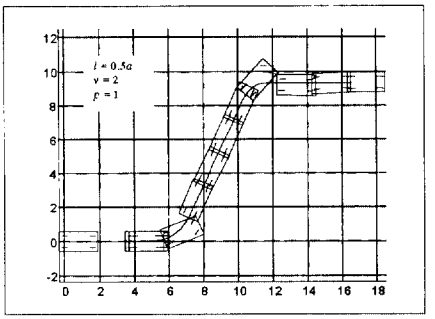

Figure 4: Look-ahead tracking

In the second case, the car-like robot is turned around and expected to move backwards to track the same trajectory with the desired velocity of $v_d = -2$m/sec. The virtual reference point is chosen at two different locations $P_1 = (l, p) = (-1.2a, -0.2)$ and $P_2 = (l, p) = (-1.2a, -0.1)$. Based on Figure 3, P_2 is closer to the vehicle symmetric axis line and able to handle more difficult maneuvers, such as the second curve, which has a higher maximum curvature change rate. The simulation results, as shown in Figure 5, show that, with $p = -0.2$, the robot fails to track the desired trajectory at the second curve, and that, with $p = -0.1$, the robot succeeds in tracking the complete desired trajectory. Our intuition and experience verify that driving a car backwards with higher steering rates will cause difficulties and even instability.

6 Conclusion

This paper analyze the stable full state tracking problem of nonholonomic wheeled mobile robots under control laws based on the input-output dynamics. It is shown that the tracking error internal dynamics and zero dynamics play a critical role of the full state tracking stability of such mobile robots. Sufficient conditions for the stable full state tracking

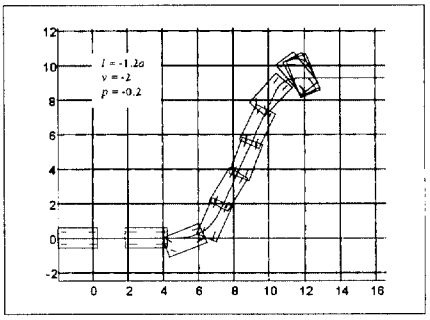

(a) $p = -0.2$

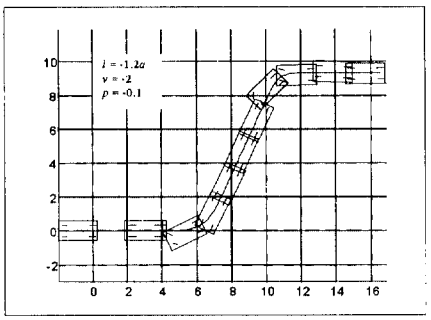

(b) $p = -0.1$

Figure 5: Look-behind tracking

offer a general approach for analysis using linear approximations. The detail investigation of a car-like mobile robot indicates that sufficient condition for stable tracking can be implemented by adjusting parameters in the output function.

References

[1] N. Sarkar, X. P. Yun, and V. Kumar, "Control of mechanical systems with rolling constraints: Applications to dynamic control of mobile robots," *The International Journal of Robotics Research*, vol. 13, pp. 55–69, Feb. 1994.

[2] C. Y. Su and Y. Stepanenko, "Robust motion/force control of mechanical systems with classical nonholonomic constraints," *IEEE Transactions on Automatic Control*, vol. 39, pp. 609–614, March 1994.

[3] G. Campion, G. Bastin, and B. d'Andréa Novel, "Structural properties and classification of kinematic and dynamic models of wheeled mobile robots," *IEEE Transactions on Robotics and Automation*, vol. 12, pp. 47–61, 1996.

[4] J. M. Yang and J. H. Kim, "Sliding mode control for trajectory tracking of nonholonomic wheeled mobile robots," *IEEE Transactions on Robotics and Automation*, vol. 15, no. 3, pp. 578–587, 1999.

[5] X. P. Yun and Y. Yamamoto, "Stability analysis of the internal dynamics of a wheeled mobile robot," *Journal of Robotic Systems*, vol. 14(10), pp. 697–709, 1997.

[6] K. S. Tsakalis and P. A. Ioannou, *Linear Time-Varying Systems Control and Adaptation.* Prentice Hall, 1993.

[7] A. Isidori, *Nonlinear Control System.* Berlin: Springer, 1989. 2nd ed.